

Daily Sea Water Temperature Forecasting Using Machine Learning Approaches

Arif ÖZBEK*¹ ORCID 0000-0003-1287-9078

¹Mechanical Engineering Department, Ceyhan Engineering Faculty, Cukurova University, Adana

Geliş tarihi: 14.02.2022 Kabul tarihi: 30.06.2022

Atıf şekli/ How to cite: ÖZBEK, A., (2022). Daily Sea Water Temperature Forecasting Using Machine Learning Approaches. Çukurova Üniversitesi, Mühendislik Fakültesi Dergisi, 37(2), 307-317.

Abstract

The efficiency of turbines in seaside nuclear or coal-fired power plants is directly proportional to sea water temperature (SWT). The cooling medium temperature is critical in the design of any power plant when considering long-term average climatic conditions. As a result, the deviation in the SWT affects the efficiency of electricity generation. Accurate SWT estimation is critical for electrical output from power plant applications in this regard. Three different data-driven models such as long short-term memory (LSTM) neural network, adaptive neuro-fuzzy inference system (ANFIS) with fuzzy c-means (FCM) and grid partition (GP) were used to perform one-day ahead short-term SWT prediction, in this paper. The analyses were performed using 5-year daily mean SWTs measured by the Turkish State Meteorological Service in Canakkale Province between 2014 and 2018. The measured data was also used to validate the data produced by the proposed techniques. Performance criteria for the techniques suggested are mean absolute error (MAE), root mean square error (RMSE) and correlation coefficient (R). With the ANFIS-FCM technique, the best outcomes for MAE, RMSE and R values were obtained as 0.113°C, 0.191°C, and 0.9994, respectively, according to daily SWT forecasting.

Keywords: LSTM, ANFIS, Sea water temperature, Power plant

Makine Öğrenimi Yaklaşımlarını Kullanarak Günlük Deniz Suyu Sıcaklığı Tahmini

Öz

Deniz kenarına kurulu nükleer veya kömürle çalışan güç santrallerinde türbin verimliliği doğrudan deniz suyu sıcaklığına (SWT) bağlıdır. Uzun vadeli ortalama iklim koşulları göz önüne alındığında, soğutma ortamı sıcaklığı herhangi bir enerji santralinin tasarımında önemli bir rol oynar. Bu nedenle elektrik üretimindeki verimlilik SWT'deki sapmadan etkilenmektedir. Bu bakımdan, doğru SWT tahmini, santral uygulamalarından elektrik çıkışı için önemli bir rol oynamaktadır. Bu çalışmada uzun kısa süreli bellek (LSTM) sinir ağı, uyarlanabilir nöro-bulanık çıkarım sistemi (ANFIS) ile bulanık c-ortalamlar (FCM) ve ızgara bölümü (GP) gibi üç farklı veri odaklı model, bir gün sonrasının tahminini gerçekleştirmek için kullanılmıştır. Analizler, 2014-2018 yılları arasında Türkiye Devlet Meteoroloji İşleri tarafından

*Corresponding author (Sorumlu yazar): Arif OZBEK, arozbek@cu.edu.tr

Çanakkale ilinde ölçülen 5 yıllık günlük ortalama SWT'ler kullanılarak gerçekleştirilmiştir. Ölçülen veriler ayrıca önerilen modeller tarafından üretilen verileri doğrulamak için kullanılmıştır. Önerilen modeller için performans kriterleri, ortalama mutlak hata (MAE), ortalama kare hata (RMSE) ve korelasyon katsayısıdır (R). ANFIS-FCM tekniği ile günlük SWT tahminine göre MAE, RMSE ve R değerleri için en iyi sonuçlar sırasıyla 0,113°C, 0,191°C ve 0,9994 olarak elde edilmiştir.

Anahtar Kelimeler: LSTM, ANFIS, Deniz suyu sıcaklığı, Güç santrali

1. INTRODUCTION

The purpose of using water in a power station is to condense steam and remove waste heat as part of the Rankine cycle. The total water requirement of the plant depends on various important factors such as production capacity, production technology, environmental and climatic conditions of the surrounding, flow rate of the cooling fluid, and cooling system of the plant [1].

There are many studies using hybrid, machine learning and time series methods to estimate some atmospheric parameters. Researchers have developed the methods that are using adaptive network-based fuzzy inference system (ANFIS) [2,3], subtractive clustering (ANFIS-SC) and grid partition (ANFIS-GP) [4], long short-term memory (LSTM) [5,6] to predict atmospheric air temperatures. The LSTM method has been applied successfully in various fields, such as forecasting of wind speed [7-9], power of wind turbine [10-12], dam displacement [13], solar irradiance [14], electricity price [15], energy production in a solar PV plant [16] and ground surface temperature [17].

There are not many studies published to specify the forecasting of the sea water temperature using machine learning techniques in literature. Attia [1] investigated the cooling water temperature effect on the nuclear power plant thermal performance. He showed that with only a one-degree Celsius increase in seawater temperature, the nuclear power plant's thermal efficiency and electricity generation decreased by 0.152% and 0.444%, respectively. Durmayaz and Söğüt [18] and Kim and Jeong [19] also analyzed the effect of cooling water temperature on the thermal efficiency of a nuclear power plant. They stated that SWT has a direct effect on the power plant efficiency. Darmawan and Yuwono [20] investigated the

effect of increasing seawater temperature which was used as a condenser cooling medium on the performance of steam turbine. Samadianfard et al. [21] estimated the hourly water temperature at different depths in a lake in their country using some computational techniques such as adaptive network-based fuzzy inference system (ANFIS), artificial neural networks (ANNs) and gene expression programming (GEP). To evaluate the performance of their computing techniques, three different statistical indicators (the root mean square error (RMSE), the mean absolute error (MAE), and the coefficient of correlation (R)) were used.

Departing from the literature review listed above, in the present study data-driven methods (ANFIS-FCM and ANFIS-GP) and a deep learning approach established on LSTM neural network were proposed to forecast one day-ahead sea water temperature from any measurement station. The 5-year daily mean SWTs measured by the Turkish State Meteorological Service at Canakkale station on the Turkey Seas between 2014 and 2018 were used as sample data. The following are some of the study's contributions to the literature:

- With the developed methods, one hour forward SWT estimation can be made at any station without providing different meteorological data and without the need for complex calculations.
- To show which of the methods used in this study gives more sensitive results, the results obtained from all methods using the same data sets were compared with each other.
- Results obtained from LSTM and ANFIS methods were analyzed and examined according to varying input variables such as epoch number, hidden layer number, and influence radius.

2. MATERIAL AND METHOD

2.1. Long Short-Term Memory (LSTM) Neural Network

The LSTM method was introduced by Park et al. [22]. LSTM is an artificial recurrent neural network (RNN) that solves issues by adding cell states or memory cells with fixed mistakes to allow errors to be replayed without losing gradients. Three different gates are present in an LSTM. An input port learns to protect the memory cell's fixed error stream from irrelevant inputs, while an output port learns to protect other units from the memory cell's irrelevant memory content.

Finally, the forget gate teaches how long the value is in the memory cell [23,24].

Figure 1 shows the LSTM layer architecture, indicating the flow of an X time series with S-length C properties (channels) across an LSTM layer. In this layered architecture, h_t is the output (also known as the hidden state), and c_t is the cell state at time step t . In order to calculate the first output and the updated cell state, the first LSTM part is utilized for the first state of the network and the early time step of the series. This block determines the output and the updated cell state c_t at time step t using the current state of the network (c_{t-1}, h_{t-1}) and the next time step of the array.

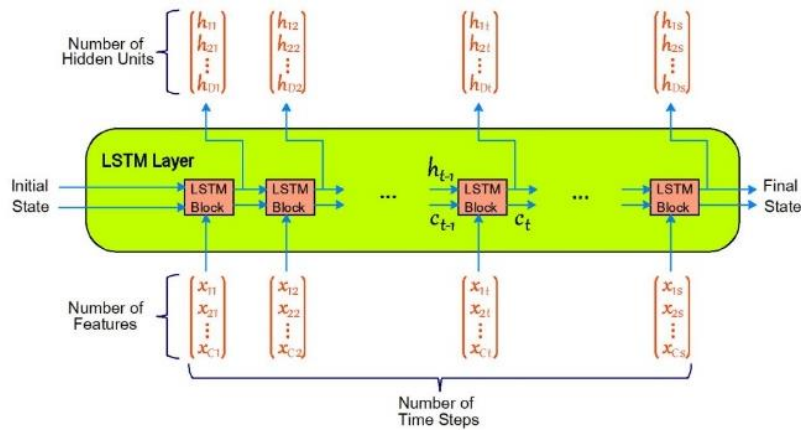


Figure 1. LSTM layer architecture

The hidden state (also known as the output state) and the cell state are both parts of the layer's state. The output of the LSTM layer for this time step is stored in the hidden state at time step t . The cell state includes information from previous time steps. At each time step, the layer performs the task of adding or removing information from the cell state. These updates are controlled using gates. Some components in the LSTM layer architecture are used to control the cell state and the hidden state of the layer. For example, input gate (i) and output gate (o) control the level of cell state update and the level of cell state added to the hidden state, respectively. Forget gate (f) checks the level of cell state reset (*forget*). On the other hand, cell candidate (g) adds the information to the cell state.

Figure 2 presents the flow of data at a time step, t . This diagram indicates how the gates forget, update, and output the cell and hidden states.

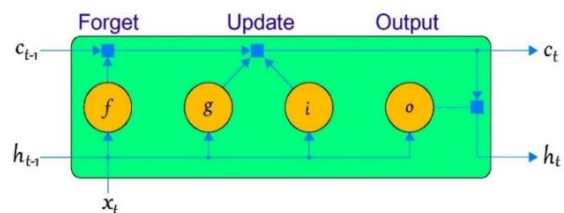


Figure 2. The flow of data at a time step, t

The input weights W , the recurrent weights R , and the bias b are called the learnable weights of an LSTM layer. The W , R , and b matrices are combinations of the input weights, recurrent

weights, and bias of each component, respectively. Detailed information about the method can be viewed from [25,26].

2.2. Adaptive Network-Based Fuzzy Inference System (ANFIS)

Adaptive Network-Based Fuzzy Inference System (ANFIS) is a universal estimator. It can be used for any true continuous function in a compact setup to any degree of accuracy. ANFIS is expressed as a network statement of Sugeno-type fuzzy systems equipped with neural learning capabilities. It creates fuzzy if-then rules with appropriate membership functions (MF) from input-output by employing a neural network learning algorithm. The FIS development procedure using the adaptive neural network framework is called ANFIS. On the other hand, general information regarding the ANFIS structure is available in the literature [27,28].

Fuzzy c-means (FCM) is a clustering method of ANFIS, allowing each data point to have multiple clusters and belonging to different membership degrees. The basis of the FCM algorithm involves minimizing the objective function. Similarly, the concept of FCM is available in the literature [28]. Grid partitioning (GP) algorithm divides the input data space into a rectangular subspace with the help of an axis-parallel partition. Each input is divided into membership functions of the same shape. The number of the fuzzy if-then rules is the same as Mn. Here, the input dimension is shown by n, and the number of partitioned fuzzy subsets for each input variable is denoted by M. This approach to solve a problem is simply referred to as functional decomposition. This phenomenon is as well extensively explained in the literature [29].

The primary distinction between linear regression and time series data is that time series data is time dependent, whereas linear regression data is assumed to be time independent. This implies that each observation is distinct from the others.

2.3. Error Analysis for the Proposed Methods

Three different statistical error criteria comprising mean absolute error (MAE), root mean square

error (RMSE), and correlation coefficient (R) are used in this study for the assessment of the goodness of a method. These error criteria are used to check the accuracy of the estimations based on the observed variables. The mathematical expressions of these error criteria are provided in Equations 1, 2, and 3, respectively.

Mean absolute error (MAE):

$$MAE = \frac{1}{N} \sum_{i=1}^N |p(i) - o(i)| \quad (1)$$

Root mean square error (RMSE):

$$RMSE = \sqrt{\frac{1}{N} \sum_{i=1}^N [p(i) - o(i)]^2} \quad (2)$$

Correlation coefficient (R):

$$R = \frac{(\sum_{i=1}^N [p(i) - \bar{p}][o(i) - \bar{o}])}{(\sqrt{\sum_{i=1}^N [p(i) - \bar{p}]^2} \sqrt{\sum_{i=1}^N [o(i) - \bar{o}]^2})} \quad (3)$$

where $p(i)$ and $o(i)$ are the predicted value and observed value at the time i , respectively. Also, \bar{p} and \bar{o} present average values of the estimated data and the actual data, respectively. The total number of data is represented by N .

3. RESULT AND DISCUSSION

The geographic coordinates of the measurement station are 40°08'29.6"N and 26°23'56.2"E. Figure 3 shows the observed SWT values with training (4 years) and testing (1 year) data to be used in the ANFIS and LSTM methods. 1460 daily sample data (blue-coloured, 80% of whole data) from 01 January 2014 to 31 December 2017 were used to train the methods and 365 daily sample data (red-coloured, %20 of the whole data) from 01 January to 31 December 2018 were used to test it. The maximum and minimum SWT's are 26.8°C and 7°C, respectively. The average value of all training and testing data is 17.1°C and the standard deviation of this data group is 5.6°C.

3.1. Fuzzy C-Means Clustering (ANFIS-FCM)

Table 1 shows the determination of optimal parameters for forecasting SWT using ANFIS-FCM. The simulation results are represented in that Table. From that table, the influence of the number of cluster nodes (membership functions = MFs) and fuzzy can be easily detected in the

results. 2 clusters (MFs) are determined as the best one that uses 5 input numbers and 100 epoch numbers. Greater cluster numbers do not yield satisfactory results owing to the non-good separation of the inputs. At the end of the simulation, MAE is 0.1131 °C and RMSE is 0.1907 °C with an R-value of 0.99943.

Table 1. Daily SWT performance forecast for the ANFIS-FCM method

Number of MFs	Input Number	Max epoch	MAE (°C)	RMSE (°C)	R
2	5	100	0.1131	0.1907	0.99943
3	5	100	0.1135	0.1908	0.99942
4	5	100	0.1156	0.2001	0.99937
5	5	100	0.1153	0.2036	0.99934
6	5	100	0.1240	0.2165	0.99926
7	5	100	0.1231	0.2140	0.99928
8	5	100	0.1178	0.2066	0.99933
9	5	100	0.1229	0.2181	0.99925
10	5	100	0.1245	0.2214	0.99923
10	5	300	0.1275	0.2193	0.99925

Figure 4-a exhibits not only the observed but also the predicted data for the 2018 year, and Figure 4-b and 4-c show observed and predicted testing data for June and October months, respectively to be able to see more detail. The regression graph of the observed data against the predicted is shown in Figure 4-d. The figure shows that the quality of the predicted data gives a good fit.

GP. The table shows the results of predicting the daily SWT using this classification method. The lowest MAE is equal to 0.1195 °C and RMSE is 0.2185 °C with an R-value of 0.99925 when using 2 clusters, 5 input numbers, and 10 epoch numbers. It can also be noted that when using two clusters and five input numbers, increasing the epoch number does not affect the results positively.

3.2. Grid Partitioning (ANFIS-GP)

Table 2 shows the determination of optimal parameters for forecasting of SWT using ANFIS-

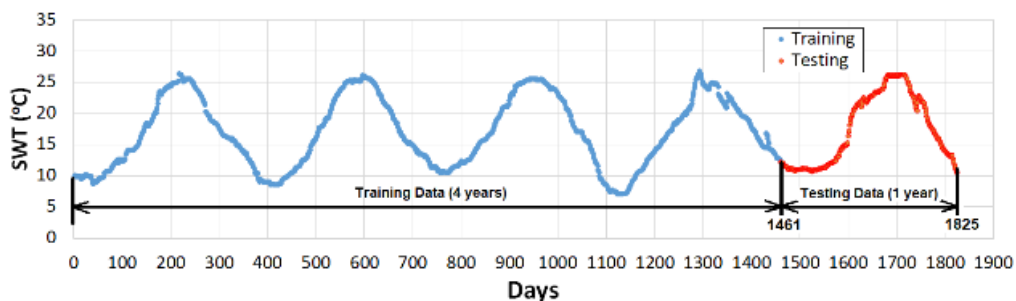


Figure 3. Observed sea water temperature time series for Canakkale, training (blue) and testing (red) data

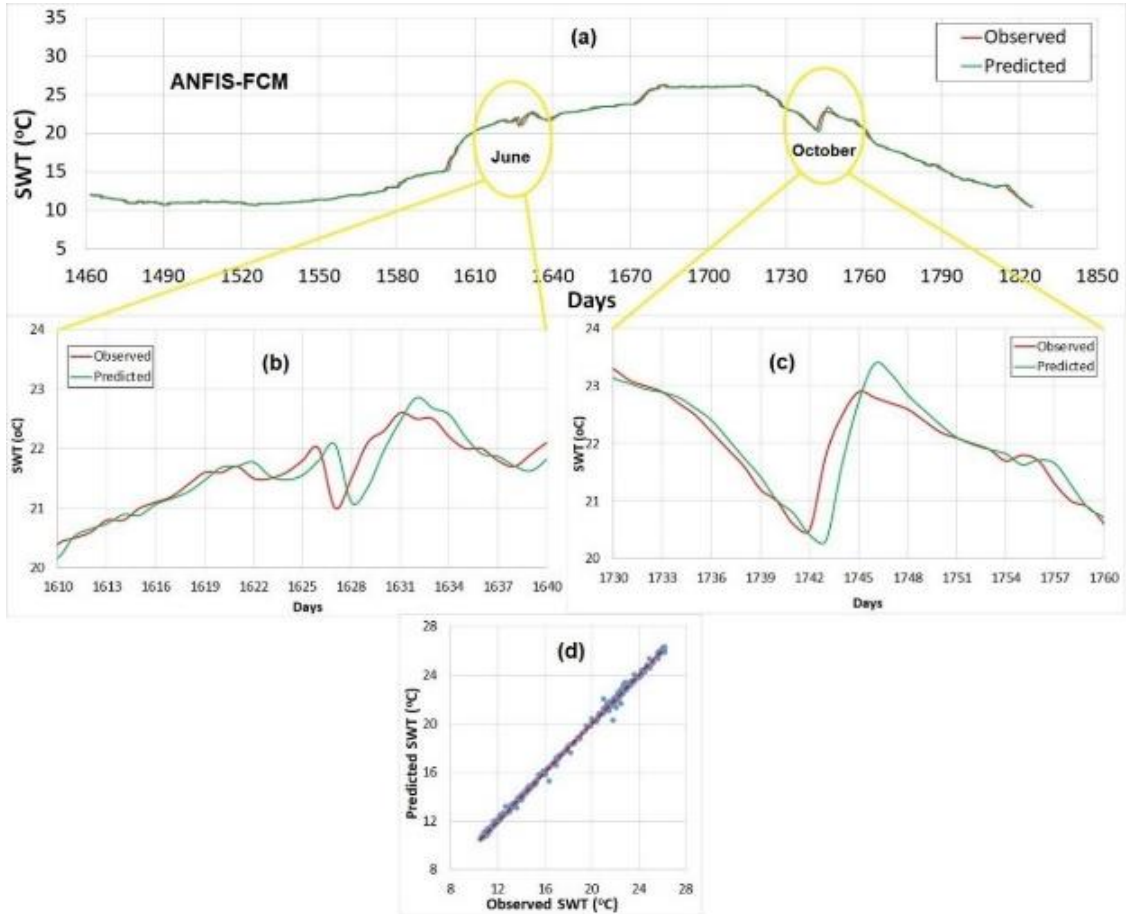


Figure 4. ANFIS with FCM clustering for observed and predicted testing data for a) whole 2018 year, b) June 2018, c) October 2018, d) the observed versus predicted data for the whole 2018 year

Table 2. Daily SWT performance forecast for the ANFIS-GP method

Number of MFs	Input Number	Max epoch	MAE (°C)	RMSE (°C)	R
2	5	10	0.1195	0.2185	0.99925
2	5	50	0.1196	0.2189	0.99925
2	5	100	0.1250	0.2361	0.99913
2	5	200	0.1456	0.2892	0.99869
2	6	50	0.1401	0.2761	0.99881
2	6	100	0.1462	0.2956	0.99864
2	7	100	0.1271	0.2883	0.99746

Figure 5 illustrates the simulation results of the ANFIS-GP method. While Figure 5-a indicates the observed and predicted testing data for the 2018 year, Figure 5-b and 5-c show observed and predicted testing data for June and October

months, respectively. Figure 5-d also displays the regression plot of the observed versus predicted data. As can be understood from the figures, the predicted and observed data are in good agreement.

3.3. Long Short-Term Memory (LSTM)

Table 3 illustrates the determination of optimal parameters for SWT forecasting using LSTM. Table points out the determination of optimal parameters for the forecasting of SWT using the LSTM method from the Canakkale station. MAE, RMSE and R-values were calculated to show the performance of the method. The influence of the hidden layer number and epoch number can be

seen in this table. 5 hidden layers and 300 epoch numbers gave the best result. The lowest MAE value is equal to 0.1295 °C and RMSE is 0.2144 °C with an R-value of 0.99927. Increasing of both the hidden layer and epoch numbers together increased the MAE and RMSE values.

Table 3. Daily SWT performance forecast for the LSTM method

Hidden Layer Number	Epoch Number	MAE (°C)	RMSE (°C)	R
5	300	0.1295	0.2144	0.99927
10	300	0.1345	0.2190	0.99924
25	300	0.1390	0.2283	0.99918
50	300	0.1653	0.2660	0.99777
50	500	0.1370	0.2247	0.99841
100	500	0.1337	0.2191	0.99924

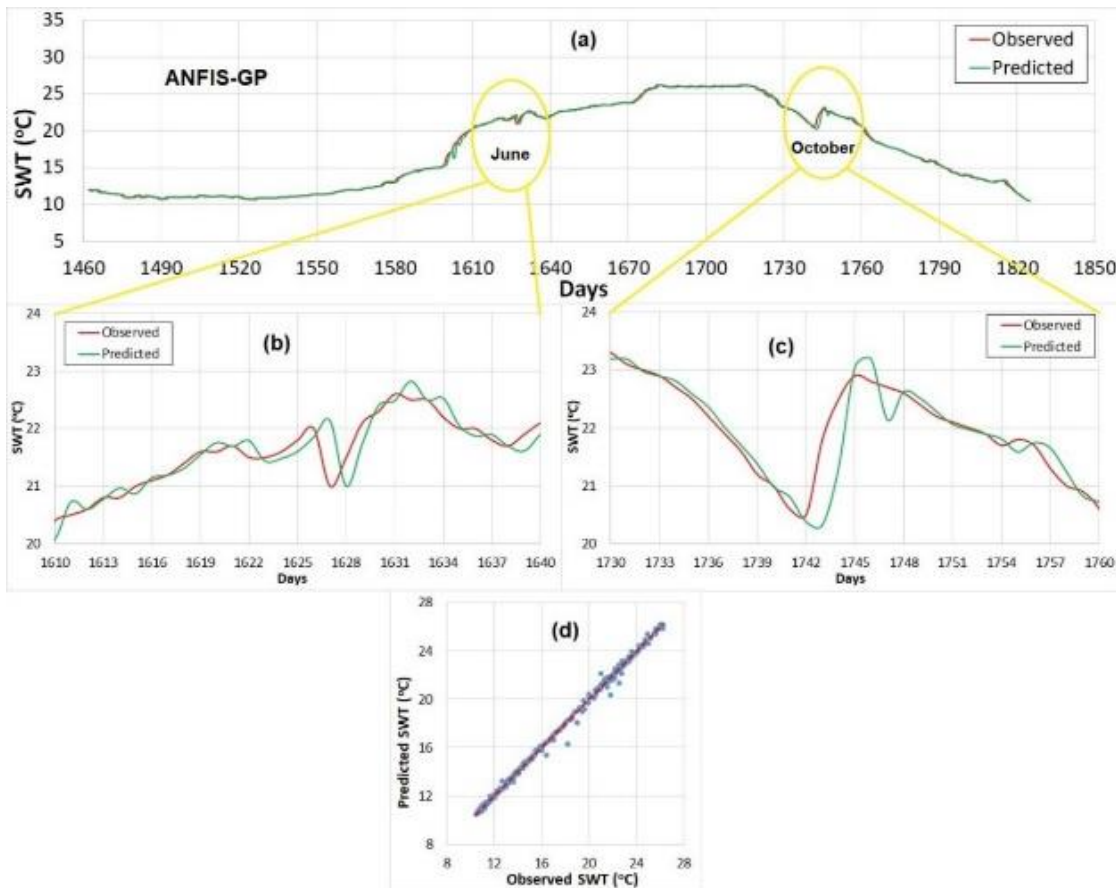


Figure 5. ANFIS with GP clustering for observed and predicted testing data for a) whole 2018 year, b) June 2018, c) October 2018, d) the observed versus predicted data for the whole 2018 year

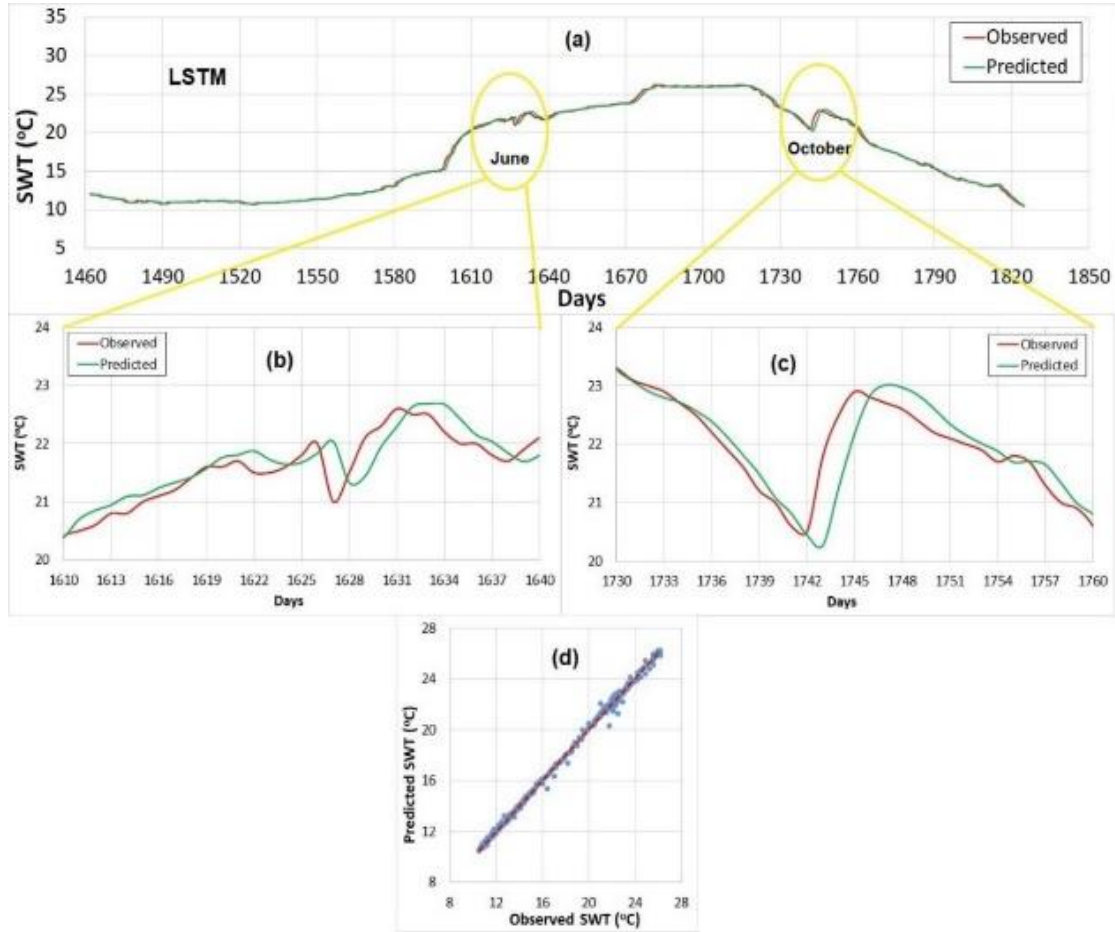


Figure 6. LSTM method for observed and predicted testing data for: a) whole 2018 year, b) June 2018, c) October 2018, d) the observed versus predicted data for the whole 2018 year

Figure 6 presents the simulation results of the LSTM method. Figure 6-a points out the observed and predicted testing data for the 2018 year and Figure 6-b and 6-c illustrate observed and predicted testing data for June and October months. Figure 6-d also displays the regression plot of the observed versus predicted data. In this figure, R value is equal to 0.99927 which indicates that the quality of the estimation results is in good fit condition.

3.4. Comparison of the Methods

The comparison was achieved to determine the most effective method of the three methods

introduced here. For this aim, the results of comparing observed and predicted daily SWT values for June and October months in the 2018 year is shown in Figure 7. In addition, for comparison, the most successful configurations that were determined in Tables 1, 2 and 3 before were evaluated. As can be seen from Table 4, the estimation ability of the ANFIS-FCM method reveals the most efficient results with an MAE value of 0.1131°C and RMSE value of 0.1907°C according to the results obtained.

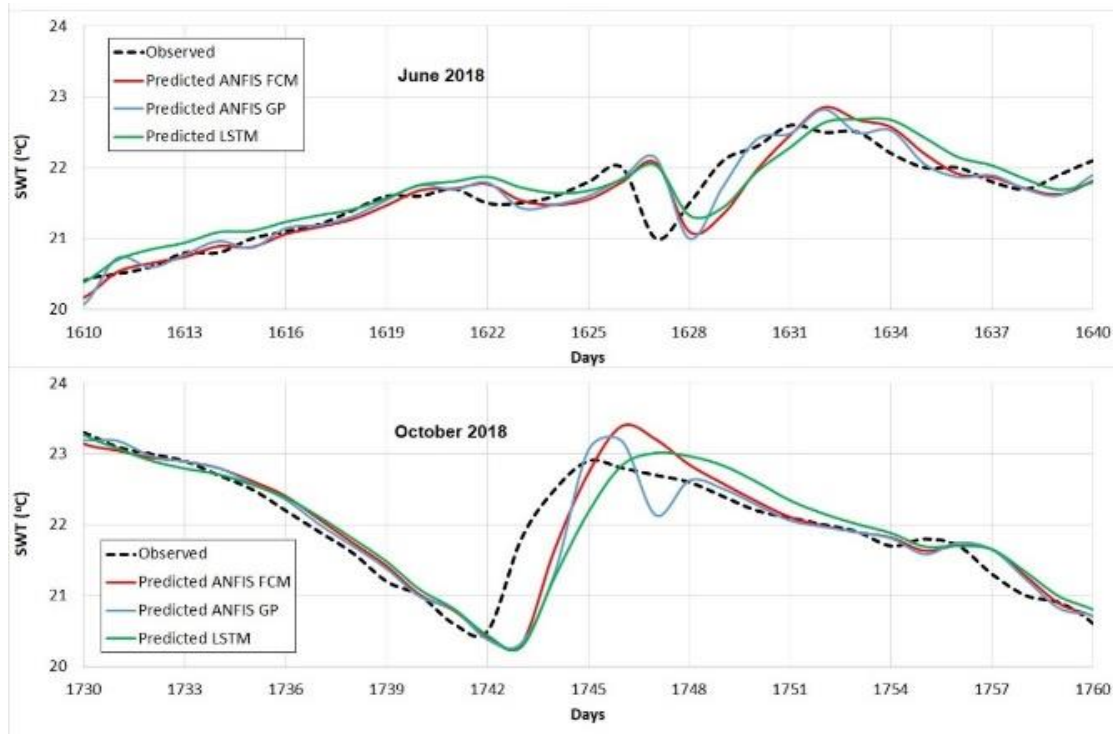


Figure 7. Comparison results of testing data for ANFIS-FCM and ANFIS-GP method with LSTM method for whole 2018 year

Table 4. Statistical accuracy results of the daily SWT forecasting

Forecasting Method	MAE (°C)	RMSE (°C)	R
ANFIS FCM	0.1131	0.1907	0.99943
ANFIS GP	0.1195	0.2185	0.99925
LSTM	0.1295	0.2144	0.99927

4. CONCLUSION

In this study, ANFIS-FCM, ANFIS-GP and LSTM neural network methods were proposed for one day-ahead forecasting of SWT.

- The RMSE values of the ANFIS-FCM, ANFIS-GP and LSTM methods were obtained as 0.1907 °C, 0.2185 °C and 0.2144 °C, respectively. It was determined that the ANFIS-FCM method gives more sensitive

forecastings than that of the ANFIS-GP and LSTM methods.

- All methods were observed to be extremely reliable and sensitive in predicting. However, the suggested ANFIS-FCM method has presented the best results in estimation performance.
- The developed method can be used to predict 1-day-ahead SWT output for any plant

without making complex calculations and providing comprehensive meteorological data.

- Future work will focus on using different deep learning functions and architectures to further improve the precision and accuracy of predictive results.

5. ACKNOWLEDGMENTS

The author would like to thank The Turkish State Meteorological Service for allowing to use of the sea water temperature data in this research. The author also thanks to the office of Scientific Research Projects of Cukurova University for funding this project under Contract no. FBA-2021-14004.

6. REFERENCES

1. Attia, S.I., 2015. The Influence of Condenser Cooling Water Temperature on the Thermal Efficiency of a Nuclear Power Plant. *Annals of Nuclear Energy*, 80, 371–378.
2. Cobaner, M., Citakoglu, H., Kisi, O., Haktanir, T., 2014. Estimation of Mean Monthly Air Temperatures in Turkey. *Comput Electron Agric*, 109 71–79.
3. Kisi, O., Shiri, J., 2014. Prediction of Long-term Monthly Air Temperature Using Geographical Inputs. *Int J Climatol*, 34, 179–186. <https://doi.org/10.1002/joc.3676>.
4. Kisi, O., Sanikhani, H., 2015. Modelling Long-term Monthly Temperatures by Several Data-driven Methods Using Geographical Inputs. *Int J Climatol*, 35, 3834–3846. <https://doi.org/10.1002/joc.4249>.
5. Ozbek, A., Sekertekin, A., Bilgili, M., Arslan, N., 2021. Prediction of 10-min, Hourly, and Daily Atmospheric Air Temperature: Comparison of LSTM, ANFIS-FCM and ARMA. *Arabian Journal of Geosciences* 14, 622. <https://doi.org/10.1007/S12517-021-06982-Y>.
6. Sekertekin, A., Bilgili, M., Arslan, N., Yildirim, A., Celebi, K., Ozbek, A., 2021. Short-term air Temperature Prediction by Adaptive Neuro-fuzzy Inference System (ANFIS) and Long Short-term Memory (LSTM) Network. *Meteorology and Atmospheric Physics* <https://doi.org/10.1007/S00703-021-00791-4>.
7. Balluff, S., Bendfeld, J., Krauter, S., 2015. Short Term Wind and Energy Prediction for Offshore Wind Farms Using Neural Networks. in: 2015, International Conference on Renewable Energy Research and Applications (ICRERA). IEEE, Palermo, 379–382. <https://doi.org/10.1109/icrera.2015.7418440>.
8. Liu, H., Mi, X., Li, Y., 2018. Wind Speed Forecasting Method Based on Deep Learning Strategy Using Empirical Wavelet Transform, Long Short Term Memory Neural Network and Elman Neural Network. *Energy Convers Manag*, 156, 498–514.
9. Chen, Zeng, J.G.Q., Zhou, W., Du, W., Lu, K., 2018. Wind Speed Forecasting Using Nonlinear-learning Ensemble of Deep Learning Time Series Prediction and Extremal Optimization. *Energy Convers Manag.*, 165, 681-695.
10. Qu, X., Xiaoning, K., Chao, Z., 2016. Short-term Prediction of Wind Power Based on Deep Long Short-term Memory. *IEEE Pes Asia-Pacific Power and Energy Engineering Conference (APPEEC)*. IEEE, 1148–1152.
11. Wu, W., Chen, K., Qiao, Y., Lu, Z., 2016. Probabilistic Short-term Wind Power Forecasting Based on Deep Neural Networks. 2016 International Conference on Probabilistic Methods Applied to Power Systems (PMAPS). Ieee, Beijing, 1–8. <https://doi.org/10.1109/pmaps.2016.7764155>.
12. López, E., Valle, C., Allende, H., Gil, E., Madsen, H., 2018. Wind Power Forecasting Based on Echo State Networks and Long Short-term Memory. *Energies* 11, 526. <https://doi.org/10.3390/en11030526>.
13. Zhang, J., Cao, X., Xie, J., Kou, P., 2019. An Improved Long Short-term Memory Model for Dam Displacement Prediction. *Math Probl Eng.*, 1-14. <https://doi.org/10.1155/2019/6792189>.
14. Qing, X., Niu, Y., 2018. Hourly Day-ahead Solar Irradiance Prediction Using Weather Forecasts by LSTM. *Energy*, 148, 461-468. <https://doi.org/10.1016/j.energy.2018.01.177>.

15. Peng, L., Liu, S., Liu, R., Wang, L., 2018. Effective Long Short-term Memory with Differential Evolution Algorithm for Electricity Price Prediction. *Energy*, 162, 1301-1314. <https://doi.org/10.1016/j.energy.2018.05.052>.
16. Ozbek, A., Yildirim, A., Bilgili, M., 2021. Deep Learning Approach for One-hour Ahead Forecasting of Energy Production in a Solar-pv Plant Energy Sources. Part a: Recovery, Utilization, and Environmental Effects, doi.org/10.1080/15567036.2021.1924316.
17. Arslan, N., Sekertekin, A., 2019. Application of Long Short-term Memory Neural Network Model for the Reconstruction of MODIS Land Surface Temperature Images. *J Atmos Solar-Terrestrial Phys*, 194, [doi:10.1016/j.jastp.2019.105100](https://doi.org/10.1016/j.jastp.2019.105100).
18. Durmayaz, A., Sogut, O.S., 2006. Influence of Cooling Water Temperature on the Efficiency of a Pressurized-water Reactor Nuclear-power Plant. *International Journal of Energy Research*, 30,799-810. [doi:10.1002/er.1186](https://doi.org/10.1002/er.1186).
19. Kim, B.K., Jeong, Y.H., 2013. High Cooling Water Temperature Effects on Design and Operational Safety of NPPS in the Gulf Region. *Nuclear Engineering and Technology*, 45(7), 961-968. [doi:10.5516/NET.03.2012.079](https://doi.org/10.5516/NET.03.2012.079).
20. Darmawan, N., Yuwono, T., 2019. Effect of Increasing Sea Water Temperature on Performance of Steam Turbine of Maura Tawar Power Plant. *Journal for Technology and Science*, 30(2), 2088-2033. (PISSN:0853-4098)
21. Samadianfard, S., Kazemi, H., Kisi, O., Liu, W.C., 2016. Water Temperature Prediction in a Subtropical Subalpine Lake Using Soft Computing Techniques. *Earth Sciences Research Journal*, 20(2) D1-D11. [doi:10.15446/esrj.v20n2.43199](https://doi.org/10.15446/esrj.v20n2.43199).
22. Park, I., Kim, H.S., Lee, J., Kim, J.H., Song, C.H., Kim, H.K., 2019. Temperature Prediction Using the Missing Data Refinement Model Based on a Long Short-term Memory Neural Network. *Atmosphere (Basel)*, 10(11), 1–16.
23. Hochreiter, S., Schmidhuber, J., 1997. Long Short-term Memory. *Neural Computation* 9(8), 1735-1780.
24. Salman, A.G., Heryadi, Y., Abdurahman, E., Suparta, W., 2018. Single Layer & Multi-layer Long Short-term Memory (LSTM) Model with Intermediate Variables for Weather Forecasting, *Procedia Comput. Sci.*, 135, 89-98.
25. Zahroh, S., Hidayat, Y., Pontoh, R.S., Santoso, A., Sukono, Bon, A.T., 2019. Modeling and Forecasting Daily Temperature in Bandung, *Proc. Int. Conf. Ind. Eng. Oper. Manag.*, (November), 406–412.
26. Liu, R., Liu, L., 2019. Predicting Housing Price in China Based on Long Short-term Memory Incorporating Modified Genetic Algorithm. *Soft Comput.*, 23(22), 11829–11838.
27. Abyaneh, H.Z., Nia, A.M., Varkeshi, M.B., Marofi, S., Kisi, O., 2011. Performance Evaluation of ANN and ANFIS Models for Estimating Garlic Crop Evapotranspiration, *J. Irrig. Drain. Eng.*, 137(5), 280–286.
28. Erduman, A.A., 2020. Smart Short-term Solar Power Output Prediction by Artificial Neural Network, *Electr. Eng.*, 102(3), 1441–1449.
29. Karakuş, O., Kuruoğlu, E.E., Altinkaya, M.A., 2017. One-day Ahead Wind Speed/power Prediction Based on Polynomial Autoregressive Model. *IET Renew. Power Gener.*, 11(11), 1430–1439.

